RNA Structure: Reading the Ribosome

Harry F. Noller

Science **309**, 1508 (2005);
DOI: 10.1126/science.1111771

Science (print ISSN 0036-8075; online ISSN 1095-9203) is published weekly, except the last week in December, by the American Association for the Advancement of Science, 1200 New York Avenue NW, Washington, DC 20005.

REVIEW

RNA Structure: Reading the Ribosome

Harry F. Noller

The crystal structures of the ribosome and its subunits have increased the amount of information about RNA structure by about two orders of magnitude. This is leading to an understanding of the principles of RNA folding and of the molecular interactions that underlie the functional capabilities of the ribosome and other RNA systems. Nearly all of the possible types of RNA tertiary interactions have been found in ribosomal RNA. One of these, an abundant tertiary structural motif called the A-minor interaction, has been shown to participate in both aminoacyl-transfer RNA selection and in peptidyl transferase; it may also play an important role in the structural dynamics of the ribosome.

As awareness of the biological importance of RNA continues to unfold, the ways in which the structural properties of RNA enable its functional capabilities are becoming all the more interesting. For more than 20 years, our understanding of RNA structure was based almost entirely on the x-ray crystal structure of the 25-kD transfer RNA (tRNA), which appeared in 1974 (*1*, *2*). The widespread lack of success in obtaining useful crystals of other RNA molecules discouraged efforts to solve new structures of more complex RNA molecules. Except for x-ray structures of the smaller hammerhead ribozyme (*3, 4*) no new RNA structures of comparable size appeared until the 160-nucleotide (nt) P4-P6 domain of the group I ribozyme, in 1996 (*5*). Only 4 years later, the first high-resolution x-ray crystal structures of the ribosomal subunits emerged (*6*–*8*), suddenly increasing information on RNA structure by two orders of magnitude (Fig. 1) (*9*, *10*). It is now possible to see directly how RNA can be folded into this breathtakingly intricate and graceful globular 2.5-MD structure containing over 4500 nt and more than 50 proteins, related versions of which are responsible for synthesis of proteins in all cells. The lessons learned from these structures not only address the function and assembly of ribosomes but provide an enormous database for interpreting and predicting the structures of the numerous other cellular RNAs and ribonucleoproteins (RNPs), giving new insights into the structural basis of RNA function as well as how life might have originated in an RNA world (*11*).

Lessons from tRNA

Many principles of RNA structure were gleaned from the structure of the 76-nt $tRNA^{Phe}_{yeast}$ (*1*, *2*). It showed that RNA forms double-helical structures with Watson-Crick base pairing but also that the presence of ribose in RNA has a profound influence on its structure. tRNA was found to contain many noncanonical base pairs, and even base triples, that allow it to fold into its unique three-dimensional structure. Inspection of its structure reveals a strong tendency for its strands to follow an A-helical path, even in non-base-paired regions. For example, hairpin turns are accomplished not by incremental bends in the RNA chain but by abrupt local changes in direction, usually centered around one or two nucleotides. A commonly observed motif is the U turn, seen in the anticodon loop of tRNA, which involves hydrogen bonding of the N3 position of a uridine with the phosphate group of a nucleotide three positions downstream, causing an abrupt reversal in direction of the RNA chain. The tRNA structure also revealed the coaxial stacking of RNA helices: The 7-base-pair (bp) acceptor stem stacks on the 5-bp T stem to form one continuous A-form helical arm of 12 bp (Fig. 2B). The other two helices, the D stem and anticodon stem, also stack, although imperfectly, to form a second helical arm. The two coaxially stacked arms form the familiar L form of tRNA (Fig. 1). Coaxial stacking is a common feature of RNA and is widespread in rRNA, where continuous coaxial stacking of as many as 70 bp is found (Fig. 2). In spite of the wealth of information provided by the 76-nt tRNA, many other common features of RNA structure were absent.

The Post-tRNA Renaissance

In the absence of new RNA crystals, nuclear magnetic resonance (NMR) spectroscopists began to solve the structures of small RNAs, quickly adding to the diversity of known RNA folding motifs (*12*). The ability of small ligands to stabilize or rearrange RNA structure was exemplified by the dramatic structural rearrangement of the HIV TAR RNA induced by binding a single arginine residue (*13*).

One of the first rRNA structures obtained by NMR spectroscopy was the sarcin-ricin loop (SRL) of 28S rRNA (*14*), a structure that interacts with elongation factors EF1 and EF2 and is targeted by the lethal ribotoxins α-sarcin and ricin. The compact 29-nt structure was found to contain several purine-purine base pairs, a tetraloop, and a bulged guanosine adjacent to a reverse Hoogsteen A-U pair. It is stabilized by stacking of bases from opposite strands (termed cross-strand stacking) and H-bonding between imino protons of guanines and phosphate oxygens. The zig-zag fold of its backbone (the S turn), along with its other features, have been identified as recurring motifs in RNA structures.

Although NMR spectroscopy sidestepped the difficult problem of crystallizing RNA, it is limited to structural analysis of molecules with an upper size limit of about that of tRNA. This led

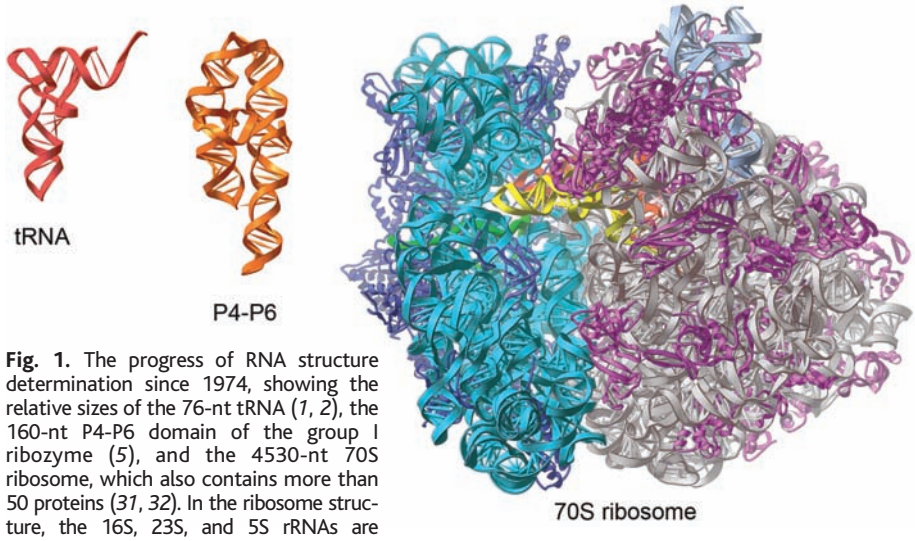

Fig. 1. The progress of RNA structure determination since 1974, showing the relative sizes of the 76-nt tRNA (*1*, *2*), the 160-nt P4-P6 domain of the group I ribozyme (*5*), and the 4530-nt 70S ribosome, which also contains more than 50 proteins (*31*, *32*). In the ribosome structure, the 16S, 23S, and 5S rRNAs are colored cyan, gray, and gray-blue, respectively, and the small and large subunit ribosomal proteins are dark blue and magenta, respectively. Two tRNAs (yellow and orange) and a mRNA (green) are visible inside the ribosome.

Center for Molecular Biology of RNA, Department of Molecular, Cell, and Developmental Biology, Sinsheimer Laboratories, University of California, Santa Cruz, Santa Cruz, CA 95064, USA.

to an increased effort to improve methods for RNA crystallization (*15*). An encouraging sign was the appearance of the first crystal structures of a catalytic RNA, the hammerhead ribozyme, solved first as an RNA-DNA chimera and subsequently as an all-RNA structure (*3*, *4*). Both structures revealed essentially the same fold, with three helices arranged in a Y configuration containing a U turn at the three-helix junction. Scott and coworkers have gone on to solve the structures of four additional constructs by using strategies that trap the hammerhead ribozyme in different states of its catalytic cycle, revealing for the first time a detailed high-resolution "movie" of the mechanism of action of a catalytic RNA (*16*). Since the hammerhead structure, crystal structures of three more ribozymes have been solved, including the hepatitis delta virus ribozyme (*17*), the hairpin ribozyme (*18*), and the group I self-splicing intron (*19*–*21*), providing the structural basis for understanding their respective catalytic mechanisms.

The first RNA structure to be solved that exceeded the size of tRNA was the 160-nt P4-P6 domain of the *Tetrahymena* group I intron at 2.8 Å resolution (*5*). It consists of two extended coaxial helical elements connected at one end by an internal loop containing a 150° bend (Fig. 1). For the first time, examples could be seen of the kinds of RNA-RNA interactions that are used to stabilize the packing of RNA helices into larger, more complex globular structures. One of these has been named the A-minor motif (*22*), one of the most abundant long-range interactions in rRNA, in which single-stranded adenosines make tertiary contacts with the minor grooves of double helices. A-minor interactions also play important functional roles. Helix-helix interactions were also formed by ribose zippers involving H bonding between the 2′-hydroxyl group of a ribose in one helix and the 2′-hydroxyl and the 2-oxygen of a pyrimidine base (or the 3-nitrogen of a purine base) of the other helix between their respective minor groove surfaces. In addition, close approach of phosphates was often mediated by bound hydrated magnesium ions. A recurring motif in the P4-P6 structure, called the A platform, positions adenines side by side in a pseudo–base pair within a helix, opening the minor groove for interactions with nucleotides from noncontiguous RNA strands.

rRNA Secondary Structure Prediction

Long before the first ribosome crystal structures appeared, the essential features of rRNA secondary structures were correctly predicted by using comparative sequence analysis (*23*–*25*). At about this same time, Michel and colleagues used a similar approach to establish the secondary structures of group I introns (*26*). Comparative analysis establishes base pairing by identification of compensating base changes in complementary nucleotides between two or more sequences. This approach was first explicitly applied by Fox and Woese (*23*), who, studying 5S rRNA sequences as phylogenetic markers, realized there was a common secondary structure that was compatible with several different sequences. Comparative analysis was used on the large 16S and 23S rRNAs from the outset; consequently, their main secondary structure features were deduced rather quickly (*24*, *25*), to be confirmed crystallographically some 20 years later. Even some rRNA tertiary interactions were discovered by comparative analysis (*27*, *28*), as had been the case earlier for tRNA (*29*). The secondary structures of most globular RNAs have been determined by comparative analysis, including ribonuclease (RNase) P RNA, the group I and group II self-splicing introns, snRNAs, and telomerase RNA. For some RNAs, such as in vitro–selected RNA aptamers and ribozymes, a lack of phylogenetic sequence information has been overcome by introducing base variation with the use of either site-directed or random mutagenesis (*30*).

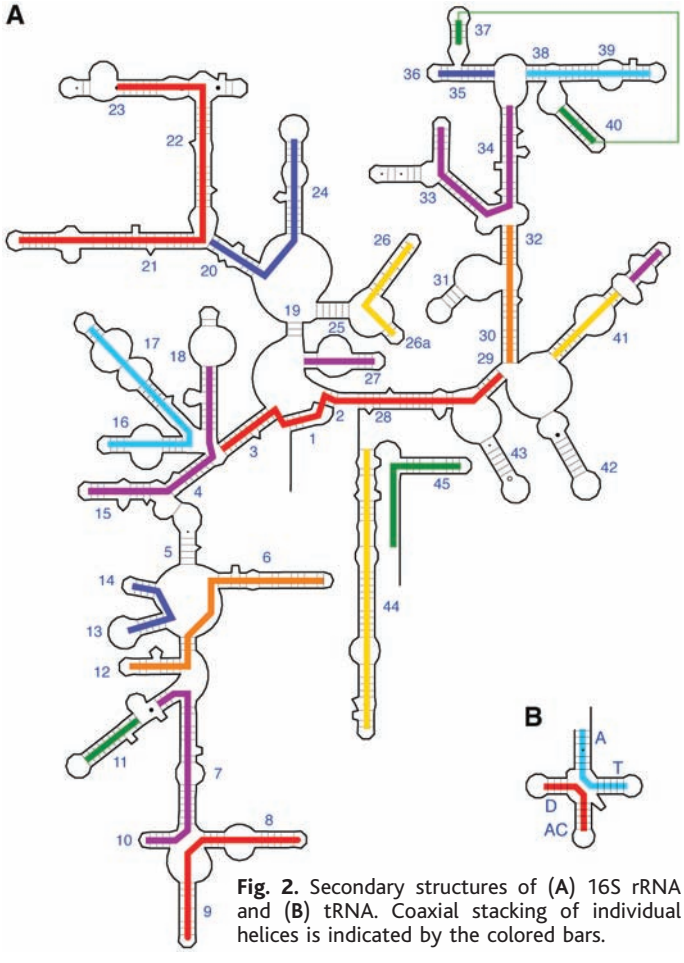

Fig. 2. Secondary structures of (**A**) 16S rRNA and (**B**) tRNA. Coaxial stacking of individual helices is indicated by the colored bars.

About 60% of the nucleotides in the large rRNAs are involved in Watson-Crick base pairing. However, the unpaired bases are not distributed evenly among the four bases. In *Escherichia coli* 16S rRNA, for example, the proportions of unpaired bases for G, C, and U are 31%, 29%, and 33%, respectively, whereas 62% of As are unpaired (*27*), a tendency that extends to other functional RNAs. The preponderance of unpaired adenosines reflects their participation in special tertiary interactions.

Implications for RNA Tertiary Structure

The ribosome and its subunits are the largest asymmetric structures that have been solved so far by crystallography. The 2.4 Å *Halocarcula marismortui* 50S subunit structure (*8*) and the ~3 Å *Thermus thermophilus* 30S subunit structure (*6*, *7*) provided the first detailed views of the molecular interactions that are responsible for the structures of both ribosomal subunits. A 5.5 Å structure of a functional complex of the *T. thermophilus* 70S ribosome revealed the positions of the tRNAs and mRNA and their interactions with the ribosome, as well as the features of the intersubunit bridges (*31*, *32*). Many co-crystals of ribosomes and subunits containing tRNA and mRNA fragments, protein factors, and antibiotics have now been solved in an effort to understand the mechanism of translation (*33*). These analyses have been complemented by extensive cryogenic electron microscopy (cryo-EM) reconstruction studies, which have led to lower-resolution structures for many functional complexes of the ribosome that have so far defied crystallization (*34*).

Many long-standing questions were immediately resolved by the crystal structures. A critical issue was whether the rRNA merely serves as a structural scaffold, or whether it is directly involved in ribosomal function. The structures showed that rRNA in fact does both of these things, creating the structural framework for the ribosome, and at the same time forming the main features of its functional sites, confirming that the ribosome is indeed a ribozyme (*35*).

It was already clear from the secondary structures of 16S and 23S rRNA that they are organized into domains of a few hundred nu-

cleotides each, four for 16S rRNA and six for 23S rRNA (*24*, *25*). The three major domains of 16S rRNA were assigned to the head, body, and platform features of the low-resolution EM structure for the 30S subunit (*36*, *37*), and this has been confirmed by crystallography (*6*, *7*). Their structural autonomy appears to facilitate their independent movement during translation. The six domains of 23S rRNA are more closely packed against one another (*8*) and were not distinguishable as separate domains of the 50S subunit at low resolution.

Comparative analysis of 16S and 23S rRNA secondary structure also provided a sense of the allowed variation in the sizes of the different helical elements (*24*, *25*, *27*). Some helices are strictly conserved in length, showing no phylogenetic variation. Others vary, showing both shorter and longer versions relative to *E. coli* in different phylogenetic branches. In some cases, shortening but not lengthening is permitted. These observations can now be interpreted in view of the three-dimensional structures. Variable-length helices are always found on the surface, distant from the functional center of the ribosome, with their extensible ends pointing into the solvent. Ones that can be shortened, but not lengthened, have ends whose maximum lengths are restricted by potential clash with other structural elements.

The hundreds of individual rRNA helices in the ribosome allow us to draw new generalities about RNA secondary structure. Most rRNA helices terminate at both ends in G-C pairs. As predicted from sequence analysis and chemical probing studies, noncanonical A-G pairs often flank the ends of helices (*38*, *39*). The crystal structures show that they are most commonly sheared A-G pairs, as well as Watson-Crick–like A-G imino pairs (*40*, *41*). As first observed for tRNA, bases that fall into nonhelical (so-called single-stranded) regions of the secondary structure are typically found to be highly structured, participating in H bonding and stacking interactions with other elements of the RNA. Of the 25 possible kinds of noncanonical base pairs involving two or more hydrogen bonds (*40*, *41*), 20 are found in the ribosome. For example, the sheared A-G pair is represented 20 times in 16S rRNA and 46 times in 23S rRNA, and there are 7 and 22 examples, respectively, of the reverse Hoogsteen A-U pair. Westhof and co-workers have made a comprehensive study of the kinds of noncanonical interactions that appear in RNA and their geometric and stereochemical classification (*42*, *43*).

Among the most interesting structural motifs are the A-minor interactions, of which hundreds of examples are found in rRNA (*22*). In these motifs, single-stranded adenosines reach into the minor groove of a helix, making both H bonding and van der Waals contacts. They are not simply base-base interactions, but nucleoside-nucleoside interactions, because crucial contacts are also made with the riboses as well as the bases (Fig. 3). Pairs of consecutive A-minor interactions are often found, in which two adjacent adenosines sequentially form type II and type I interactions (although some type II interactions are also made by guanosines) with adjacent base pairs (Fig. 3, A and B), which are typically G-C pairs. Although they form many important structural contacts, they are also intimately involved in ribosome function. For example, the 3′-terminal adenosines of both the A- and P-site tRNAs are positioned in the peptidyl transferase site by A-minor interactions with 23S rRNA (*35*). An elegant RNA-based mechanism using the A-minor motif occurs in the decoding site of the 30S subunit (*44*), where the stereochemical fit of codon-anticodon pairing is monitored by A-minor interactions between A1492 and A1493 of 16S rRNA (supported by additional interactions from G530) and the minor groove surface of the codon-anticodon helix (Fig. 3, C to E). The prevalence of A-minor interactions in rRNA helps to account for the overrepresentation of single-stranded adenosines in rRNA secondary structures.

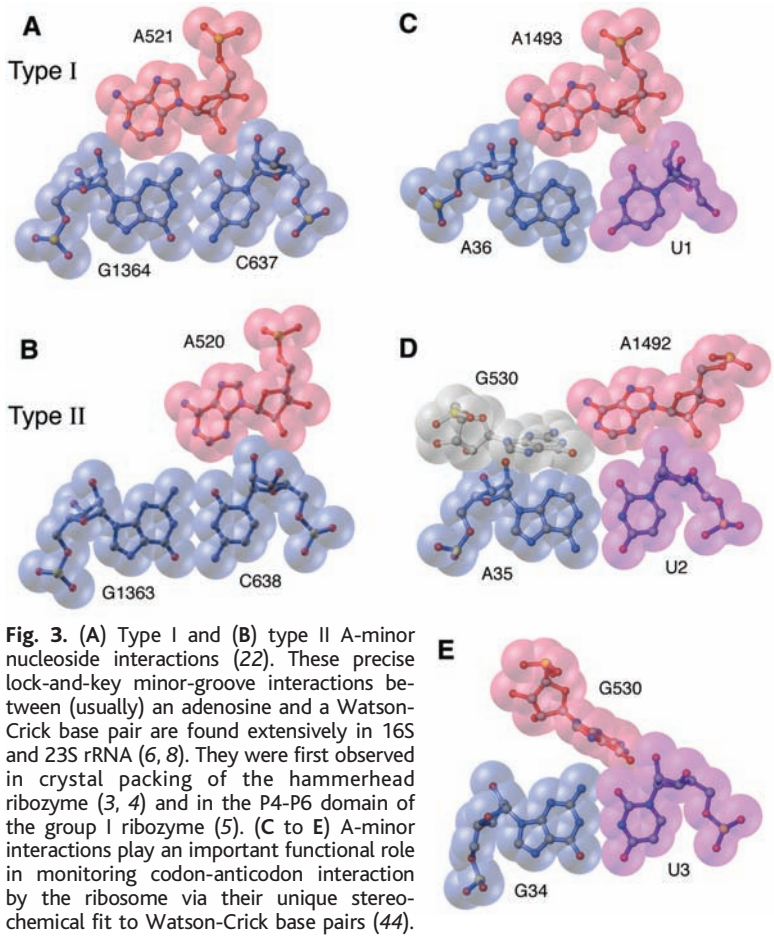

Fig. 3. (**A**) Type I and (**B**) type II A-minor nucleoside interactions (*22*). These precise lock-and-key minor-groove interactions between (usually) an adenosine and a Watson-Crick base pair are found extensively in 16S and 23S rRNA (*6*, *8*). They were first observed in crystal packing of the hammerhead ribozyme (*3*, *4*) and in the P4-P6 domain of the group I ribozyme (*5*). (**C** to **E**) A-minor interactions play an important functional role in monitoring codon-anticodon interaction by the ribosome via their unique stereochemical fit to Watson-Crick base pairs (*44*).

About half of the helices in rRNA terminate in hairpin loops. In *T. thermophilus* 16S rRNA, 17 of its 32 hairpin loops are tetraloops (Fig. 2), first identified as the most common type of hairpin loop in rRNA by inspection of their phylogenetically derived secondary structures (*45*). As found for many RNAs, the GNRA tetraloop is most common in rRNA, representing about half of the observed tetraloops. The other hairpin loops use a variety of strategies to execute their turns. In 16S rRNA, there are five examples of U turns, and G turns are also found, in which the stabilizing hydrogen bond to the backbone phosphate is made from the N1 position of a guanine base; these include the G turns that are an intrinsic feature of GNRA tetraloop structures. Indeed, G(N1)-phosphate H bonds are widespread, making many kinds of base-backbone interactions in addition to G turns, of which there are dozens of examples in both 16S and 23S rRNA.

It has been said that "tRNA looks like Nature's attempt to make RNA do the job of a protein" (*46*). rRNA takes this notion to the extreme, representing the limit of what can be done to make a globular, functional molecule out of RNA, beyond which nature has resorted to proteins. The basic building block of RNA structure, the double helix, greatly restricts the ability of RNA to form globular structures because of its rigidity and limited geometry. How then, does RNA manage to form a structure such as the ribosome, with its complex, curving three-dimensional surfaces, stereospecific binding pockets, and other intricate molecular features? Almost all rRNA helices contain seven or fewer contiguous Watson-Crick base pairs, in spite of the fact that the overall dimensions of the ribosome (~250 Å) would in principle allow for continuous heli-

ces of as many as 80 bp. A general strategy found throughout the ribosome is to connect these short helices by bulge loops or internal loops of unequal length, introducing bends that allow a high degree of structural curvature. The connecting loops themselves are highly structured, rich in noncanonical base pairs as well as base-phosphate and base-ribose interactions that constrain the geometries of the individual bends. Indeed, bases that are not involved in either Watson-Crick or some kind of noncanonical interaction are very rare, explaining why so few bases are reactive toward chemical probes and their inability to hybridize with oligonucleotide probes. Some of the connecting loop features have been recognized as recurring motifs in RNA structure: for example, the S turn motif and the kink turn that creates a sharp 120° angle between two adjacent helices (*47*).

These irregular compound helices are packed against one another to form the final globular structure. Earlier, it was thought that RNA-RNA packing would be mediated by the basic ribosomal proteins to alleviate charge repulsion between the high density of negatively charged phosphate groups lining the RNA backbone. It was therefore surprising to find extensive regions of closely packed RNA helices containing little or no protein. Packing of RNA structural elements is of special interest in the functional sites, which are mostly devoid of proteins. In fact, ribosomal proteins are found mainly on the outer surface of the ribosome, although many of them contain long, unstructured tails that penetrate the RNA (*48*, *49*). Not surprisingly, both divalent and monovalent cations as well as polyamines, which have long been known to be essential for the structural and functional integrity of ribosomes, mediate RNA-RNA packing interactions in the ribosome, helping to neutralize phosphate-phosphate repulsion (*50*). The ribose zipper (*5*) is yet another strategy that is used for packing the minor grooves of rRNA helices against each other.

Folding of RNA differs in many ways from that of proteins. There are only four types of nucleotide monomers; there are six backbone torsion angles, instead of two; and RNA structure is not nucleated by a hydrophobic core, as are most proteins. Instead, RNA folding uses the two principle devices that were first seen in the double-helical structures of DNA and RNA: hydrogen bonding and base stacking.

An example of how noncanonical H-bonded interactions can direct the packing of RNA helices is the helix 6–helix 8 interaction in 16S rRNA (*6*) (Fig. 4). These two helices pack against each other at a 90° angle, via their respective minor-groove surfaces. They are positioned by two layers of coplanar bases that form two exquisitely stereospecific H-bonded networks. Both layers contain central A-minor interactions in which adenosines in helix 8 bind to receptors in helix 6, forming the heart of the interhelical connection. The upper (yellow) layer is formed by interaction of the minor-groove side of a Watson-Crick G-C pair in helix 6 through a type II A-minor interaction with the adenosine of a noncanonical Hoogsteen base pair in helix 8. The lower (red) layer is formed from a noncanonical A-G-G base triple, of which one of the guanosines forms the receptor for a Type I A-minor interaction from an adenosine involved in a noncanonical A-C pair in helix 8. The positions of both of the A-minor adenosines are constrained by their additional base-base interactions, tightly restricting the overall geometry. It seems counterintuitive that this apparently coplanar arrangement of bases results in a 90° packing angle between the two helices. This is the result of three effects: first, the bases of RNA helices are tilted at an angle to the helical axis; second, the adenine bases in A-minor interactions typically form ~30° angles with the planes of their receptor bases; and third, the adenines are held at an angle to helix 8 by additional noncanonical base-base interactions.

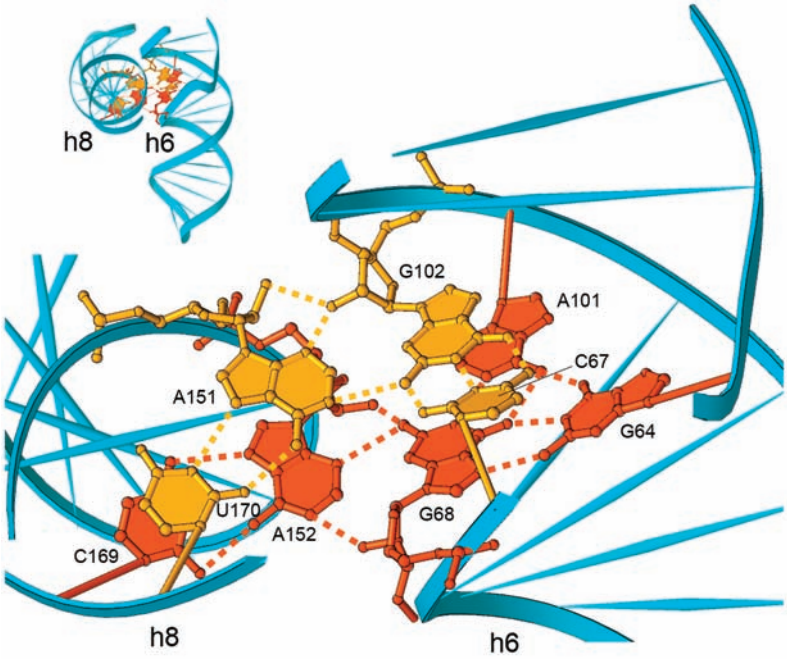

Fig. 4. An example of how the ribosome packs two helices (h6 and h8) in 16S rRNA together at right angles to each other (*6*). Two layers of nucleotides (yellow and red) form extensive hydrogen-bonded networks (dotted lines) that precisely locate the two helices. In the top (yellow) layer, nucleotide A151 in h8 makes a type II A-minor interaction with the G102-C67 base pair in h6, itself bolstered by a Hoogsteen pair with U170. In the bottom (red) layer, A152 of h8 makes a type I A-minor interaction with a Watson-Crick-like pair between G68 and A101 of h6. Both A152 and its A-G receptor are bolstered by additional noncanonical base pairings with C169 and G64.

In addition to coaxial stacking of helices, the ribosome contains some remarkable examples of base stacking of unpaired bases, such as in the noncanonical structure known as helix 70 in 23S rRNA (Fig. 5). Helix 70 is located at the subunit interface of the 50S subunit near the geometric center of the ribosome (*8*). It forms the attachment point for helix 69, which interacts with both the A- and P-site tRNAs, as well as forming a bridge to the decoding site of 16S rRNA (*31*, *32*). Its compact, 23-nucleotide structure is a tour de force of noncanonical complexity and is one of the most conserved features of rRNA. It contains no fewer than four systems of stacked bases, one of which is bifurcated to form a short fifth stack. Although helix 70 superficially resembles a normal RNA helix, it in fact contains only a single canonical Watson-Crick base pair (G1964-C1934). Although its role in translation is not known, the projection of bases A1966 and U1944 into the minor grooves of the functionally important helices 93 and 92, respectively, are suggestive of some relationship to the peptidyl transferase activity of the ribosome.

rRNA folds correctly only by assembling with ribosomal proteins, which appear to stage the order of folding of rRNA during ribosome assembly to avoid losing improperly folded ribosomes in kinetic traps. Their role in translational function appears to be subordinate to that of rRNA, helping to improve the efficiency and accuracy of mechanisms that are based on RNA. This view is supported by their location mainly on the exterior of the ribosome, away from the functional subunit interface region (*6*–*8*, *31*, *32*). Further evidence comes from the observation that at least one-third of the ribosomal proteins can be deleted singly without conferring a lethal phenotype (*51*). Nearly all ribosomal proteins interact directly with rRNA, and few have contact with other ribosomal proteins. They are typically small and basic, representing a diverse collection of structural types that span the range of known protein folds, giving the

impression that they were recruited to the ribosome in many independent evolutionary events. As mentioned above, some ribosomal proteins have long, unstructured tails that penetrate, and co-assemble with, the rRNA (*48*, *49*). The C-terminal tails of proteins S9 and S13 contact the anticodon stem loop of tRNA in the 30S P site; cells in which the S9 and S13 tails have been deleted are viable, showing that these interactions are not essential for ribosome function (*52*). In keeping with their diverse structures, their rRNA binding sites are comparably diverse, comprising both helical and loop features; unlike DNA-binding proteins, ribosomal proteins mainly recognize higher-order structural features of rRNA, rather than base sequence (*48*, *49*). Binding to rRNA helices occurs preferentially on their minor-groove surfaces. Apart from contributing to the neutralization of negative charges on the rRNA backbone, ribosomal proteins are known to stabilize certain tertiary folds (*53*) and to help fix the relative orientation of helices at multihelix junctions (*54*). Indeed, proteins may have initially evolved to extend the structural repertoire of RNA in an RNA world (*55*).

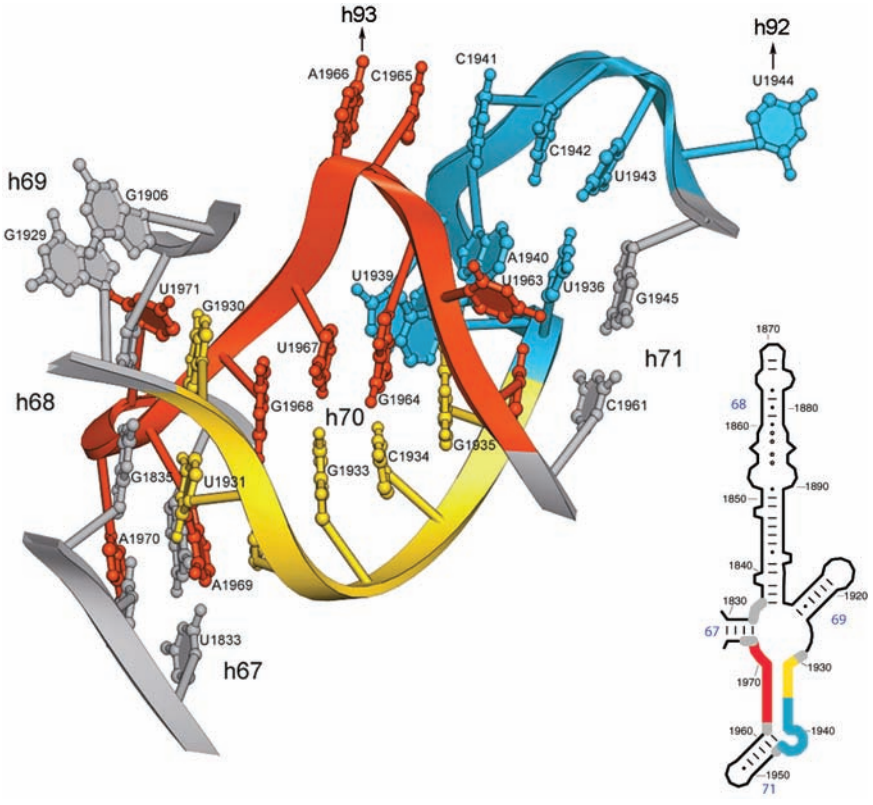

Fig. 5. Helix 70 of 23S rRNA (*8*) contains four different systems of stacked bases and contains only a single canonical Watson-Crick base pair (G1964-C1934). Its structure positions U1944 and A1966 to interact with the minor grooves of helices 92 and 93 in the peptidyl transferase region of the 50S subunit.

Ribosome Dynamics

Ribosomes are molecular machines, whose moving parts enable the dynamic process of translation. Each tRNA traverses a distance of more than 130 Å from the time it enters the ribosome as an aminoacyl-tRNA until it is released as a deacylated tRNA (*31*, *32*, *56*); it was anticipated that such large-scale tRNA movement must be matched by corresponding movements in the ribosome. Evidence for this, ranging from local conformational changes to relative movement of the 30S and 50S subunits, comes from structural changes that are observed between different crystal structures (*31*, *32*, *44*, *57*–*59*) and from cryo-EM studies of ribosomes trapped in different functional states (*34*, *60*, *61*).

An example of a local rearrangement is the flipping of bases G530, A1492, and A1493 in the 30S decoding site to monitor the accuracy of codon-anticodon interaction (*44*) (Fig. 3, C to E). Accompanying this local change is a larger-scale movement, in which the 30S subunit goes from an open to a closed conformation that is induced by binding of a cognate tRNA (*44*, *62*, *63*). It is believed that the energy derived from binding the cognate tRNA compensates for the energetic costs of the transition to the closed form. The altered conformation of the 30S subunit may affect the interactions between the aminoacyl-tRNA·EF-Tu· guanosine triphosphate (GTP) ternary complex and the conserved sarcin-ricin loop of 23S rRNA in the 50S subunit, leading to acceleration of GTP hydrolysis and accommodation of aminoacyl-tRNA (*62*, *63*).

An example of a larger-scale movement is that of the L1 arm of the 50S subunit. Exit of the E site–bound deacylated tRNA is obstructed by protein L1 and the extended arm of 23S rRNA to which it is bound (*32*). In addition, the observed contact with the elbow of tRNA bound in the P/E state (*64*) requires movement of the L1 arm by about 20 Å (*65*). In the *Dinococcus radiodurans* 50S crystal structure (*59*), the position of the L1 arm is shifted downward by about 20 Å relative to that seen in the *T. thermophilus* crystal and the *E. coli* cryo-EM structures, sufficient to allow release of the tRNA.

Coupled movement of tRNA and mRNA occurs during the EF-G–catalyzed process of translocation, the most dynamic of ribosomal functions. Translocation takes place in at least two steps, the first of which mainly involves movement of the acceptor arms of tRNA relative to the 50S subunit. This results in tRNAs bound in hybrid states, in which their anticodon ends remain in their original positions in the A and P sites of the 30S subunit while their acceptor ends move to the P and E sites of the 50S subunits (*64*). In the second step, the anticodon ends move to the P and E sites of the 30S subunit, coupled to movement of the mRNA, completing the translocation of tRNA from the A to P and P to E sites. Structural changes accompanying translocation have been analyzed by comparison of cryo-EM reconstructions in which ribosomes were trapped in the pre- and post-translocation states (*60*, *61*). Pretranslocation or posttranslocation ribosomes, containing peptidyl-tRNA bound to the A site or P site, respectively, were bound with EF-G and a nonhydrolyzable GTP analog or guanosine diphosphate (GDP). These experiments show structural differences between the pre- and posttranslocation states of the ribosome corresponding to a rotational movement of about 6° between the 30S and 50S subunits, causing relative displacements of as much as 20 Å at their extremities. This movement is accompanied by other structural changes, including rearrangement of intersubunit bridge contacts between the head of the 30S subunit and the central protuberance of the 50S subunit, as well as a 20 Å displacement of the L1 arm. On the basis of these observations, Frank and co-workers have proposed a ratchet model for translocation, in which rotational movement between the subunits and movement of the L1 arm, coupled with alternate binding and release of the two ends of the tRNA, is used to drive movement of tRNA and mRNA through the ribosome (*60*, *61*). GTP hydrolysis is coupled to translocation under normal cellular conditions, although the first step of translocation leading to formation of hybrid states can proceed spontaneously in vitro after peptide bond formation (*64*). Furthermore, the observation that a complete single round of highly accurate

translocation can proceed in the absence of EF-G and GTP, stimulated by the antibiotic sparsomycin (*66*), indicates that translocation is an inherent property of the ribosome itself.

Although the resolution of cryo-EM reconstructions is insufficient to draw detailed conclusions about the mechanism of translocational dynamics, it is likely to be yet another function of rRNA. A puzzle is how large-scale movements, such as those of translocation, which must occur at the rate of about 20 per second, avoid the potential kinetic barriers that would be expected from making and breaking of the many molecular interactions that maintain the precise geometry of the different conformational states needed for accurate translation. Helical switches, in which certain RNA sequences alternate between two different structures by base pairing with different complementary strands, have two disadvantages. First, disruption of an RNA helix has a high energy of activation, and second, it leads to single-stranded intermediates that lack the necessary rigidity to maintain precise geometry. Helical switches have not been found in ribosomes, perhaps for these reasons. The ideal dynamic interactions would thus be ones whose disruption and formation have relatively low activation barriers, maintain their local conformations in the disrupted state, and form with precise stereochemistry. The abundant A-minor interactions fit this description well. We have already seen that they participate in dynamic yet precise interactions in aminoacyl-tRNA selection and in the peptidyl transferase active site (Fig. 3) (*35*, *44*). The crystallographic evidence suggests that involvement of A-minor interactions in ribosomal dynamics may be much more widespread.

The 3.0 Å crystal structure of the isolated 30S subunit shows that there are about 55 A-minor interactions, or potential A-minor interactions, in 16S rRNA (Fig. 6). They are typically found in consecutive pairs consisting of a type II interaction followed by a type I interaction. The vast majority of them are long-range interactions; i.e., they connect parts of the secondary structure that lie in different domains or subdomains of the RNA. In contrast, the other base-base and base-backbone tertiary interactions are overwhelmingly local (*67*). Most intriguing is that eight of the sets of A-minor examples in Fig. 6 have optimal geometries except that the adenosines are out of contact range from their putative helical receptors. This suggests that these eight sets of potential A-minor contacts could play a role in the conformational dynamics of the 30S subunit. Direct support for formation of one of them comes from the electron density map of the *T. thermophilus* 70S ribosome (*32*), in which the potential interaction between helix 13 and helix 44 (Fig. 6) is clearly formed. Intriguingly, most of these potentially dynamic interactions are positioned immediately adjacent to features of 16S rRNA that form intersubunit bridges (Fig. 6) (*32*); this observation is consistent with their possible involvement in translocation, in which molecular rearrangements at the subunit interface are known to occur (*60*, *61*).

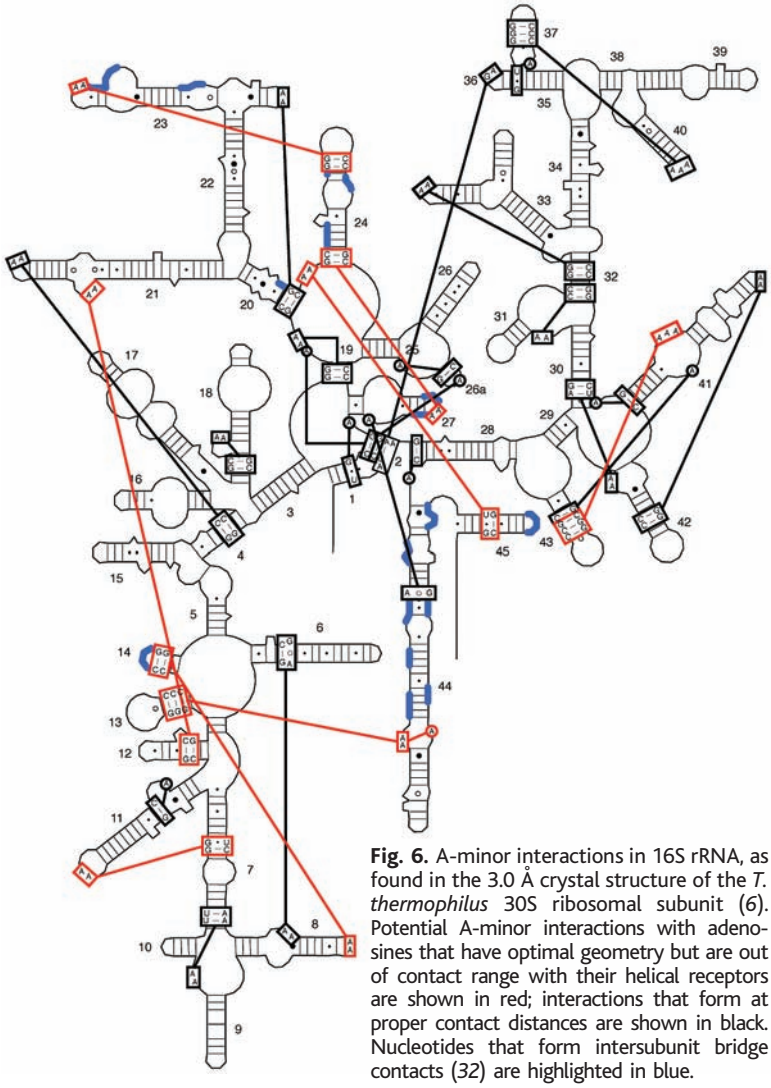

Fig. 6. A-minor interactions in 16S rRNA, as found in the 3.0 Å crystal structure of the *T. thermophilus* 30S ribosomal subunit (*6*). Potential A-minor interactions with adenosines that have optimal geometry but are out of contact range with their helical receptors are shown in red; interactions that form at proper contact distances are shown in black. Nucleotides that form intersubunit bridge contacts (*32*) are highlighted in blue.

Conclusions

We have now seen enough RNA structures to infer some generalities about what we can expect to find in other RNAs. We have probably seen most, if not all of the possible local RNA folding motifs (*10*); U turns, T loops, S turns, kink turns, hook turns, A minor interactions, A platforms, and tetraloops are all recurring features of the structures of globular RNAs. Together with the A-form double helix and the more than 20 types of noncanonical base pairs, we can now say that these comprise the building blocks of RNA architecture. It has been shown that we can already predict with good accuracy the occurrence of many of these structural features with the use of only sequence information. With the availability of many thousands of rRNA sequences plus examples of their high-resolution crystal structures, it may be possible to further extend the rules for prediction of RNA structure by using sophisticated bioinformatic approaches. Lastly, and most importantly, the ribosome is a dynamic structure, no doubt facilitated by the inherent flexibility of its RNA. The functional capabilities of a number of cellular RNAs, including the hammerhead ribozyme, group I intron, and spliceosomal RNAs also appear to depend on their structural dynamics (*68*). There is little doubt that the ribosome will continue to help us understand the strategies by which RNA structure enables movement and biological function.

References and Notes

1. J. D. Robertus *et al.*, *Nature* **250**, 546 (1974).
2. S. H. Kim *et al.*, *Science* **185**, 435 (1974).
3. H. W. Pley, K. M. Flaherty, D. B. McKay, *Nature* **372**, 68 (1994).
4. W. G. Scott, J. T. Finch, A. Klug, *Cell* **81**, 991 (1995).
5. J. H. Cate *et al.*, *Science* **273**, 1678 (1996).
6. B. T. Wimberly *et al.*, *Nature* **407**, 327 (2000).
7. F. Schluenzen *et al.*, *Cell* **102**, 615 (2000).
8. N. Ban, P. Nissen, J. Hansen, P. B. Moore, T. A. Steitz, *Science* **289**, 905 (2000).
9. V. Ramakrishnan, *Cell* **108**, 557 (2002).
10. P. B. Moore, T. A. Steitz, *Annu. Rev. Biochem.* **72**, 813 (2003).
11. R. F. Gesteland, T. R. Cech, J. F. Atkins, Eds., *The RNA World* (Cold Spring Harbor Laboratory Press, Cold Spring Harbor, NY, ed. 2, 1999).
12. O. C. Uhlenbeck, A. Pardi, J. Feigon, *Cell* **90**, 833 (1997).
13. J. D. Puglisi, R. Tan, B. J. Calnan, A. D. Frankel, J. R. Williamson, *Science* **257**, 76 (1992).
14. A. A. Szewczak, P. B. Moore, Y. L. Chang, I. G. Wool, *Proc. Natl. Acad. Sci. U.S.A.* **90**, 9581 (1993).
15. J. A. Doudna, C. Grosshans, A. Gooding, C. E. Kundrot, *Proc. Natl. Acad. Sci. U.S.A.* **90**, 7829 (1993).
16. Movie is available online (http://chemistry.ucsc.edu/~wgscott/pubs/movies2.html).

17. A. R. Ferre-D'Amare, K. Zhou, J. A. Doudna, *Nature* **395**, 567 (1998).
18. P. B. Rupert, A. R. Ferre-D'Amare, *Nature* **410**, 780 (2001).
19. P. L. Adams, M. R. Stahley, A. B. Kosek, J. Wang, S. A. Strobel, *Nature* **430**, 45 (2004).
20. F. Guo, A. R. Gooding, T. R. Cech, *Mol. Cell* **16**, 351 (2004).
21. B. L. Golden, H. Kim, E. Chase, *Nat. Struct. Mol. Biol.* **12**, 82 (2005).
22. P. Nissen, J. A. Ippolito, N. Ban, P. B. Moore, T. A. Steitz, *Proc. Natl. Acad. Sci. U.S.A.* **98**, 4899 (2001).
23. G. W. Fox, C. R. Woese, *Nature* **256**, 505 (1975).
24. C. R. Woese *et al.*, *Nucleic Acids Res.* **8**, 2275 (1980).
25. H. F. Noller *et al.*, *Nucleic Acids Res.* **9**, 6167 (1981).
26. F. Michel, A. Jacquier, B. Dujon, *Biochimie* **64**, 867 (1982).
27. R. R. Gutell, B. Weiser, C. R. Woese, H. F. Noller, *Prog. Nucleic Acid Res. Mol. Biol.* **32**, 155 (1985).
28. R. R. Gutell, H. F. Noller, C. R. Woese, *EMBO J.* **5**, 1111 (1986).
29. M. Levitt, *Nature* **224**, 759 (1969).
30. R. Green, A. D. Ellington, J. W. Szostak, *Nature* **347**, 406 (1990).
31. J. H. Cate, M. M. Yusupov, G. Z. Yusupova, T. N. Earnest, H. F. Noller, *Science* **285**, 2095 (1999).
32. M. Yusupov *et al.*, *Science* **292**, 883 (2001).
33. For example, (*57*, *69*, *70*).
34. J. Frank, *Biopolymers* **68**, 223 (2003).
35. P. Nissen, J. Hansen, N. Ban, P. B. Moore, T. A. Steitz, *Science* **289**, 920 (2000).
36. H. F. Noller, C. R. Woese, *Science* **212**, 403 (1981).
37. R. Brimacombe, P. Maly, C. Zwieb, *Prog. Nucleic Acid Res. Mol. Biol.* **28**, 1 (1983).
38. D. Moazed, S. Stern, H. F. Noller, *J. Mol. Biol.* **187**, 399 (1986).
39. T. Elgavish, J. J. Cannone, J. C. Lee, S. C. Harvey, R. R. Gutell, *J. Mol. Biol.* **310**, 735 (2001).
40. M. E. Burkard, D. H. Turner, I. Tinoco Jr., in (*11*), pp. 675–685.
41. W. Saenger, *Principles of Nucleic Acid Structure* (Springer-Verlag, New York, 1984).
42. N. B. Leontis, E. Westhof, *Curr. Opin. Struct. Biol.* **13**, 300 (2003).
43. A. Lescoute, N. B. Leontis, C. Massire, E. Westhof, *Nucleic Acids Res.* **33**, 2395 (2005).
44. J. M. Ogle *et al.*, *Science* **292**, 897 (2001).
45. C. R. Woese, S. Winker, R. R. Gutell, *Proc. Natl. Acad. Sci. U.S.A.* **87**, 8467 (1990).
46. F. H. C. Crick, *Cold Spring Harb. Symp. Quant. Biol.* **31**, 3 (1966).
47. D. J. Klein, T. M. Schmeing, P. B. Moore, T. A. Steitz, *EMBO J.* **20**, 4214 (2001).
48. D. E. Brodersen, W. M. Clemons Jr., A. P. Carter, B. T. Wimberly, V. Ramakrishnan, *J. Mol. Biol.* **316**, 725 (2002).
49. D. J. Klein, P. B. Moore, T. A. Steitz, *J. Mol. Biol.* **340**, 141 (2004).
50. D. J. Klein, P. B. Moore, T. A. Steitz, *RNA* **10**, 1366 (2004).
51. E. R. Dabbs, *J. Bacteriol.* **140**, 734 (1979).
52. L. Hoang, K. Fredrick, H. F. Noller, *Proc. Natl. Acad. Sci. U.S.A.* **101**, 12439 (2004).
53. S. Stern, T. Powers, L.-M. Changchien, H. F. Noller, *Science* **244**, 783 (1989).
54. J. W. Orr, P. J. Hagerman, J. R. Williamson, *J. Mol. Biol.* **275**, 453 (1998).
55. H. F. Noller, *RNA* **10**, 1833 (2004).
56. R. K. Agrawal *et al.*, *J. Cell Biol.* **150**, 447 (2000).
57. A. P. Carter *et al.*, *Science* **291**, 498 (2001); published online 4 January 2001 (10.1126/science.1057766).
58. H. F. Noller, A. Baucom, *Biochem. Soc. Trans.* **30**, 1159 (2002).
59. J. Harms *et al.*, *Cell* **107**, 679 (2001).
60. J. Frank, R. K. Agrawal, *Nature* **406**, 318 (2000).
61. M. Valle *et al.*, *Cell* **114**, 123 (2003).
62. J. M. Ogle, F. V. Murphy, M. J. Tarry, V. Ramakrishnan, *Cell* **111**, 721 (2002).
63. J. M. Ogle, A. P. Carter, V. Ramakrishnan, *Trends Biochem. Sci.* **28**, 259 (2003).
64. D. Moazed, H. F. Noller, *Nature* **342**, 142 (1989).
65. H. F. Noller, M. M. Yusupov, G. Z. Yusupova, A. Baucom, J. H. Cate, *FEBS Lett.* **514**, 11 (2002).
66. K. Fredrick, H. F. Noller, *Science* **300**, 1159 (2003).
67. Global searches for RNA tertiary interactions, including A-minor interactions, in 16S (4) and 23S (6) rRNA were carried out by using CASTER (*71*).
68. E. A. Doherty, J. A. Doudna, *Annu. Rev. Biochem.* **69**, 597 (2000).
69. L. Ferbitz, T. Maier, H. Patzelt, B. Bukau, E. Deuerling, N. Ban, *Nature* **431**, 590 (2004).
70. J. L. Hansen, J. A. Ippolito, N. Ban, P. Nissen, P. B. Moore, T. A. Steitz, *Mol. Cell* **10**, 117 (2002).
71. CASTER, A. Baucom, Univ. California Santa Cruz, 2005.
72. I thank A. Baucom for preparation of molecular graphics figures and W. G. Scott for discussions. Work in the author's laboratory was supported by grants from the NIH and the NSF. H.N. is a paid member of the scientific advisory board of and owns equity in the biopharmaceutical company Rib-X, which is involved in antibiotic development.

10.1126/science.1111771

REVIEW

From Birth to Death: The Complex Lives of Eukaryotic mRNAs

Melissa J. Moore

Recent work indicates that the posttranscriptional control of eukaryotic gene expression is much more elaborate and extensive than previously thought, with essentially every step of messenger RNA (mRNA) metabolism being subject to regulation in an mRNA-specific manner. Thus, a comprehensive understanding of eukaryotic gene expression requires an appreciation for how the lives of mRNAs are influenced by a wide array of diverse regulatory mechanisms.

Many written accounts of eukaryotic gene expression might start something like this: "Messenger RNAs (mRNAs) are the central conduits in the flow of information from DNA to protein. In eukaryotes, mRNAs are first synthesized in the nucleus as pre-mRNAs that are subject to 5′-end capping, splicing, 3′-end cleavage, and polyadenylation. Once pre-mRNA processing is complete, mature mRNAs are exported to the cytoplasm, where they serve as the blueprints for protein synthesis by ribosomes and then are degraded." Like a short obituary, however, this dry and simplistic description captures nothing of the intricacies, intrigues, and vicissitudes defining the life history of even the most mundane mRNA. In addition, of course, some mRNAs lead lives that, if not quite meriting an unauthorized biography, certainly have enough twists and turns to warrant a more detailed nucleic acid interest story. It is these intricacies, and our recent progress in understanding them, that are the subject of this review. We will follow the lives of eukaryotic mRNAs from the point at which they are birthed from the nucleus until they are done in by gangs of exonucleases lying in wait in dark recesses of the cytoplasm. Along the way, mRNAs may be shuttled to and from or anchored at specific subcellular locations, be temporarily withheld from the translation apparatus, have their 3′ ends trimmed and extended, fraternize with like-minded mRNAs encoding proteins of related function, and be scrutinized by the quality-control police. Although some of these processes were originally thought to affect only select mRNA populations or be largely limited to highly specialized cell types like germ cells and neurons, recent work suggests that the majority of mRNAs in multiple cell types are subject to a diverse array of regulatory activities affecting essentially every aspect of their lives.

Department of Biochemistry, Howard Hughes Medical Institute, Brandeis University, 415 South Street, Waltham, MA 02454. E-mail: mmoore@brandeis.edu

The mRNP as a Posttranscriptional Operon

Throughout their lifetimes, mRNAs are escorted by a host of associated factors, some of which remain stably bound while others are subject to dynamic exchange (Table 1). Together with mRNA, this complement of proteins and small noncoding RNAs [e.g., microRNAs (miRNAs)] constitute the messenger ribonucleoprotein particle (mRNP). It is the unique combination of factors accompanying any particular mRNA, as well as their relative positions along the transcript, that dictates almost everything that happens to that mRNA in the cytoplasm. In budding yeast, it is estimated that ~570 different proteins have the capacity to bind RNA (*1*). This number is no doubt considerably larger in humans, because a single type of RNA binding domain, the RNA recognition motif (RRM), is represented in